2019 19th International Conference on Micro and Nanotechnology for Power Generation and Energy Conversion Applications (PowerMEMS) 978-1-7281-5638-5/20/$31.00 ©2020 IEEE 10.1109/PowerMEMS49317.2019.92321112648

Energy harvesting and wireless power transfer in a unified system for wearable devices

Binh Duc Truong[1], Caleb Roundy[2], Robert Rantz[1] and Shad Roundy[1]

[1]Department of Mechanical Engineering, [2]Department of Bioengineering, University of Utah, Salt Lake, UT, 84112 USA

E-mail: Binh.D.Truong@utah.edu

Abstract. This paper presents a device concept that allows us to utilize the coils of an electromagnetic vibration-based energy harvester as a receiver for a magnetic resonant coupled wireless power transfer system (WPTS), with focus on low-power wearable applications. The parasitic capacitances of the coils along with their inductances form a single equivalent receiver coil configured in parallel. This self-resonance characteristic relaxes the requirement of adding an additional capacitor and still retains the system inherent simplicity. Measurements with an arbitrarily chosen load resistance of $R_{\mathrm{L}} = 100\ \Omega$ demonstrate a generated power of $\sim 397.4\ \mu$W at a distance between the transmitter and receiver of 2 cm at a root mean square applied $\mathbf{B}-$field of $200\,\mu$T, approximately.

1. Introduction

Wireless power transfer and energy harvesting systems offer promising means for powering sensing networks, as alternatives to traditional batteries [1]. They become an indispensable breakthrough in the Internet of Things, which is changing human life in the 21^{th} century [2]. Both methods can play vital roles in electronic devices, depending on particular circumstances. For instance, while vibrational harvesters are widely used in wearable devices to scavenge energy from human motion [3], inductive wireless power transfer provides more potential in implantable bioelectronics applications [4].

The primary technologies for harvesting energy from the human body for wearables are thermoelectric generators and inertial kinetic harvesters [1]. The low and irregular frequency of human motion is a challenge for the effective implementation of inertial harvesters which are typically designed for resonance at higher frequencies. Therefore, non-resonant transducers or magnetic plucking configurations for frequency up-converting devices may be used to overcome this challenge [5]. Recently, Rantz *et. al.* have proposed a structure using a sprung eccentric rotor for an electromagnetic rotational energy harvester [6]. The prototype, with optimal spring stiffness and electrical load, could generate a maximum average power of 61.3 μW, which was about 5 times higher than that of the unsprung counterpart under same excitation condition [7].

Near-field wireless power transfer (i.e., which includes inductive and capacitive resonantly coupled systems) has become a prominent research topic in the last decade [8]. WPTS has played a significant role in the development of implantable sensors and is commercially available [4]. However, the application of WPTS to wearable devices has attracted less attention. As

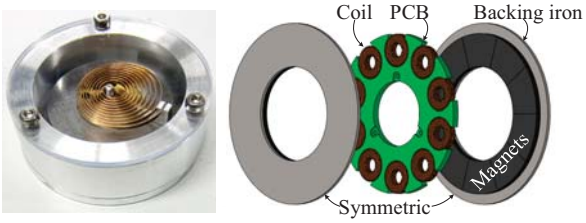

Figure 1: The device prototype used in experiments and a close-up view of the coil arrangement inside.

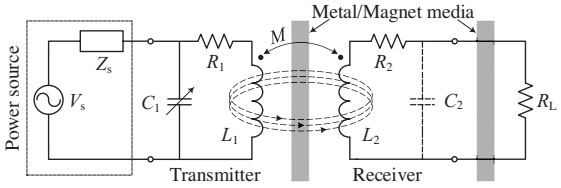

Figure 2: An illustration of the two-coil WPTS concept.

technology improves, using wearable self-powered health monitoring systems offers significant potential to improve health and quality of life. Therefore, the need for long-term, sustainable power sources for wearable health monitoring systems is increasing.

This work opens the possibility of combining inertial energy harvesting and WPTS in the same device, whereby both methods can support each other depending on specific situations. Since the harvesting scheme has previously been proven to be efficient, the concept using parallel-parallel resonant coupled WPTS will be investigated and performed in the presence of metallic plates (i.e., the device case). The main aim here is to demonstrate the device concept. Other issues such as modeling and power (or efficiency) optimization are not objectives of this paper and are open for future investigations.

2. Device concept and analysis

The details of the device structure (i.e., a dual eccentric rotor, a torsional spring, five magnet pole-pairs, back-iron shield in each rotor and coils) as well as the energy scavenging mode are presented in [7]. Figure 1 shows the prototype used for measurements and the arrangement of ten copper coils connected in series placed in a PCB that is fixed to the housing. When excited by human motion, the relative displacement between the rotor magnets and the PCB induces an voltage on the coils, converting the mechanical energy to an electrical form that is delivered to a load resistance in series with the coils. In the analysis of inertial energy harvesters, the inductance and parasitic capacitance of each coil are typically neglected since the rotation frequency is much lower than 100 Hz. The coils form a single equivalent inductor whose self-resonant frequency is in the range of hundreds of kHz or MHz. This frequency range is suitable for implementing a resonantly coupled WPTS without any modifications or additional components. The WPTS then becomes an alternative to the energy harvesting approach and ensures the continuity of delivering power to the electronics.

Figure 2 depicts a schematic of the circuit model for the two-coil WPTS, where ten copper coils within the device are represented by a receiver coil with inductance L_2, parasitic capacitance C_2 and stray resistance R_2. The transmitter coil L_1 can be freely designed and connected to a variable capacitor C_v in parallel (not shown in Figure 2) for frequency matching. Let C_1 be the sum of the parasitic capacitance C_p (of the transmitter L_1) and C_v, i.e., $C_1 = C_\mathrm{p} + C_\mathrm{v}$. In order to determine the anti-resonance angular frequency, ω_r, of each coil, we consider their impedance

$$Z_\mathrm{c} = \left[\frac{1}{j\omega C}(j\omega L + R)\right] \Big/ \left[\frac{1}{j\omega C} + j\omega L + R\right] \tag{1}$$

and set the imaginary part equal to zero

$$\Im\{Z_\mathrm{c}\} = \frac{-\omega(\omega^2 L^2 C + R^2 C - L)}{(\omega^2 LC - 1)^2 + (\omega RC)^2} = 0, \tag{2}$$

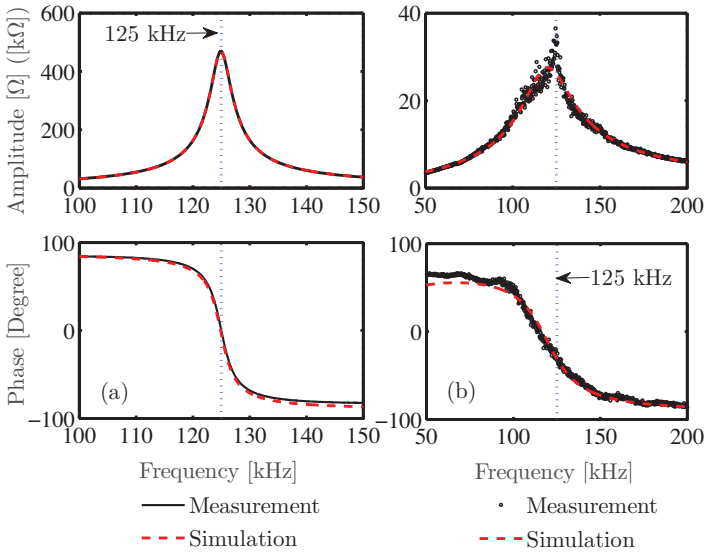

Figure 3: Measured and simulated impedance amplitude and phase of (a) the transmitter and (b) the receiver. The additional capacitance C_1 is tuned to match the anti-resonance frequency of the two coils. The impedance amplitude of the transmitter/receiver is in Ω/kΩ respectively.

which yields

$$\omega_{\mathrm{r}} = \sqrt{\frac{1}{LC} - \left(\frac{R}{L}\right)^2} = \frac{1}{L}\sqrt{\frac{L}{C} - R^2} = \frac{1}{\tau_{\mathrm{L}}}\sqrt{\frac{\tau_{\mathrm{L}}}{\tau_{\mathrm{C}}} - 1} \tag{3}$$

where $\tau_{\mathrm{L}} = L/R$, $\tau_{\mathrm{C}} = RC$, ω is the drive angular frequency and RLC represents for both $R_1L_1C_1$ and $R_2L_2C_2$. For the resonant coupled WPTS, C_1 is tuned so that the anti-resonance angular frequencies of the transmitter and receiver coils are identical ${}^{\mathrm{T}}\omega_{\mathrm{r}} = {}^{\mathrm{R}}\omega_{\mathrm{r}} = \omega_0$. It should be noted that ω_{r} is slightly different from the resonance angular frequency of the series-series configuration expressed by [9]

$$\omega_{\mathrm{s}} = 1/\sqrt{LC} = 1/\sqrt{\tau_{\mathrm{L}}\tau_{\mathrm{C}}}. \tag{4}$$

In addition, the maximum impedance amplitude is achieved at

$$\omega^* = \frac{1}{L}\sqrt{\frac{L}{C}\sqrt{1 + 2\frac{R^2C}{L}} - R^2} = \frac{1}{\tau_{\mathrm{L}}}\sqrt{\frac{\tau_{\mathrm{L}}}{\tau_{\mathrm{C}}}\sqrt{1 + 2\frac{\tau_{\mathrm{C}}}{\tau_{\mathrm{L}}}} - 1} \tag{5}$$

where ω^* is the stationary point of $|Z_{\mathrm{c}}|$, determined by $\mathrm{d}|Z_{\mathrm{c}}|/\mathrm{d}\omega = 0$. In the case where $\tau_{\mathrm{C}} \ll \tau_{\mathrm{L}}$, we get $\omega_{\mathrm{s}} \approx \omega^* \approx \omega_{\mathrm{r}}$. The closed-form of ω_{r} and ω^* are essential for system design and optimization in future work. For the purpose of evaluating the system performance, the receiver is commonly connected to a load resistance R_{L}.

In practice, we use a network analyzer to measure the impedances of these coils separately before mounting them into a complete system to avoid any dynamic interference. Firstly, the obtained maximum impedance-amplitude of the receiver is marked at 125 kHz. Then, the variable capacitor at the transmitter side is adjusted to tune its impedance peak to 125 kHz as well. The two anti-resonance frequencies of the transmitter and receiver coils are now close to each other in order to form a resonantly coupled system, as can be seen in Figures 3. The impedance phases are correspondingly shown in the same Figure for a complete set of the measured data. The coil inductance, capacitance and resistance of the transmitter and receiver are estimated based on a numerical least-square optimization scheme. All of the parameters, along with the anti-resonance frequency $f_{\mathrm{r}} = \omega_{\mathrm{r}}/2\pi$ and the extreme frequency $f^* = \omega^*/2\pi$, are listed in Table 1. The simulation results predicted by formula (1) are in good agreement with those of experiments.

Table 1: Coil Parameters. T - Transmitter, R - Receiver

T/R	C_1, nF	L_1, μH	R_1, Ω	${}^{\mathrm{T}}f_{\mathrm{r}}$, kHz	${}^{\mathrm{T}}f^*$, kHz	C_2, pF	L_2, mH	R_2, kΩ	${}^{\mathrm{R}}f_{\mathrm{r}}$, kHz	${}^{\mathrm{R}}f^*$, kHz
Value	91.28	17.78	0.42	124.88	124.93	205.04	8.55	1.56	116.66	120.11

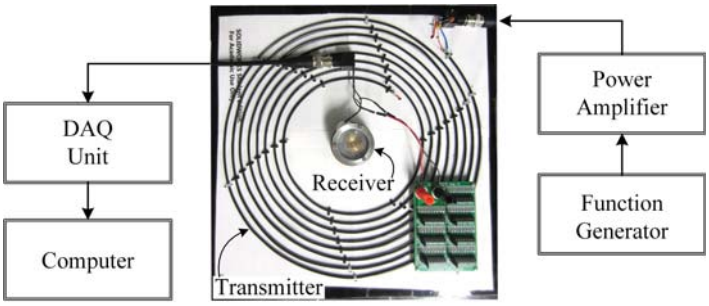

Figure 4: Schematic of the experimental setup.

3. Measurement results

When a lossy dielectric material is close to a resonator, its quality factor decreases and the resonance frequency is shifted, as observed in [10]. In the case under consideration, the receiver coil is covered by a more complex, but similar, structure of metallic and magnetic materials. Therefore, the same effect is expected to occur. For a simple and symmetric system (i.e., both the receiver and transmitter are designed to be identical), when the receiver is blocked by only one metal plate, one solution is to place another plate symmetrically in the transmitting side [10]. Another method, using a slotted metal plate to eliminate eddy currents, was reported in [11]. In this work, we choose to adjust the variable capacitor connected to the transmitter coil instead in order to match the resonance frequencies of the two resonators, as presented in Section 2.

A schematic of the experimental setup is presented in Figure 4. A function generator is used to alter the input signals for a power amplifier, including drive frequency and control voltage, which is denoted as V_{S} and is a peak-to-peak value. The output voltage across the load is collected by a data acquisition unit connected to a computer for further processing. The root-mean-square magnetic flux density generated by the transmitter coil is measured by an AC milligauss meter. The applied $\mathbf{B}-$field can be expressed by a function of V_{S} as $B_{\mathrm{rms}} \approx 0.51 V_{\mathrm{S}}$, fitted from the experimental results.

Figure 5a shows the frequency responses of the WPTS with different values of B_{rms}. The DAQ internal resistance is first used as an electrical load for convenience, $R_{\mathrm{L}} = 1$ MΩ. The

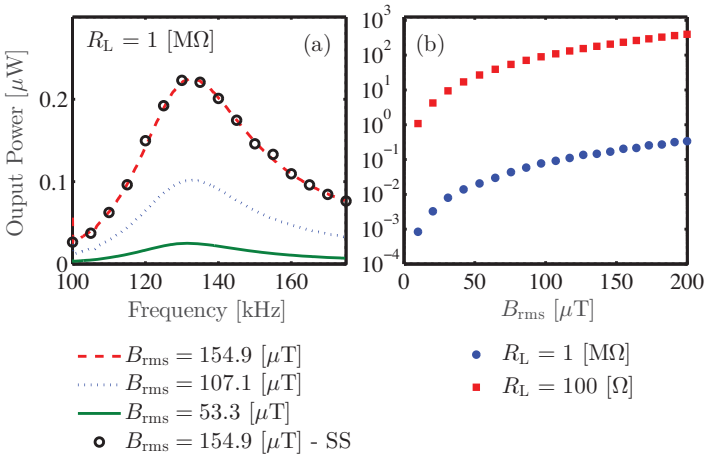

Figure 5: (a) Frequency responses of the WPTS with $R_{\mathrm{L}} = 1$ MΩ and various values of the input control voltage V_{S}. Notation: SS - steady state. (b) Variation of the output power with respect to the input applied magnetic flux density B_{rms} for different load resistance R_{L} at fixed drive frequency $f = 125$ kHz.

measurements are conducted by using swept signals within the range of 100 and 175 kHz, and the time duration of $\Delta t = 10$ s. The power delivered to the load increases with $B_{\rm rms}$ as expected. However, the optimal frequency is slightly different from the anti-resonance of each coil under the effect of the coupled condition, about 133.1 kHz instead of 125 kHz. We also investigate the steady-sate responses of the system with discrete drive frequencies at $B_{\rm rms} = 154.9\,\mu$T (or $V_{\rm S} = 300$ mV equivalently). The obtained results are identical to those of corresponding swept-frequency measurements, demonstrating that the impact of the sweep rate can be neglected. This observation helps to reduce the workload of the experiments without compromising the accuracy of measured data (i.e., use of swept-frequency signals rather than discrete ones).

Figure 5b shows the transferred power as a function of $B_{\rm rms}$ for two load resistance, 1 MΩ and 100 Ω, at a fixed frequency of 125 kHz. The maximum output power of 397.4 μW is achieved with a 100 Ω resistance at $B_{\rm rms} = 200\,\mu$T, which is much higher than that of $R_{\rm L} = 1$ MΩ. This highlights a requirement of adding impedance matching circuits to optimize the generated power for each specific loading condition. Figure 5b also demonstrates that power output is a quadratic function of $B_{\rm rms}$ as expected.

4. Concluding remarks

We have performed an experimental study of a concept that utilizes the coils of an inertial electromagnetic energy harvester as a receiver for a two-coil resonantly-coupled WPTS. We also successfully demonstrated the possibility of wireless power transfer despite the complexity of the structure with the presence of metallic plates covering the receiver coil. This is a preliminary analysis that raises the potential of bringing together two different methods (energy harvesting and wirelessly transferring power) into a single device. This extends the operational capability of the unified system either in the two cases with or without human motion during the daily activities. The influence of the metallic plates on the resonator's performance and optimization problems are of interest for future considerations.

Acknowledgment

This work was supported by the National Science Foundation ASSIST Nanosystems ERC under Award Number EEC-1160483.

References

[1] Mitcheson P 2010 Energy harvesting for human wearable and implantable bio-sensors *IEEE EMBC* pp 3432–3436
[2] Hassan Q, Khan A and Madani S 2017 *Internet of Things: Challenges, Advances, and Applications* Chapman & Hall/CRC Computer and Information Science Series (CRC Press) ISBN 9781351651059
[3] Lockhart R, Janphuang P, Briand D and de Rooij N F 2014 A wearable system of micromachined piezoelectric cantilevers coupled to a rotational oscillating mass for on-body energy harvesting *2014 IEEE 27th International Conference on Micro Electro Mechanical Systems (MEMS)* pp 370–373 ISSN 1084-6999
[4] Agarwal K, Jegadeesan R, Guo Y X and Thakor N V 2017 *IEEE Reviews in Biomedical Engineering* **10** 136–161 ISSN 1937-3333
[5] Spreemann D, Manoli Yand Folkmer B and Mintenbeck D 2006 *Journal of Micromechanics and Microengineering* **16** S169–S173
[6] Rantz R, Halim M A, Xue T, Zhang Q, Gu L, Yang K and Roundy S 2018 *Smart Materials and Structures* **27** 044001
[7] Halim M, Rantz R, Zhang Q, Gu L, Yang K and Roundy S 2018 *Applied Energy* **217** 66 – 74 ISSN 0306-2619
[8] Song M, Belov P and Kapitanova P 2017 *Applied Physics Reviews* **4** 021102 (*Preprint*)
[9] Sample A P, Meyer D T and Smith J R 2011 *IEEE Transactions on Industrial Electronics* **58** 544–554 ISSN 0278-0046
[10] Yu X, Skauli T, Skauli B, Sandhu S, Catrysse P B and Fan S 2013 *AIP Advances* **3** 062102 (*Preprint*)
[11] Kim J H and Ahn C 2018 *IEEE Antennas and Wireless Propagation Letters* **17** 587–590 ISSN 1536-1225